Materials Research. 2024; 27:e20220282
DOI: https://doi.org/10.1590/1980-5373-MR-2022-0282

Wear Analysis of Plasma Sprayed Calcium and Strontium Zirconates on Inconel 718

G. Venkatesh[a]*, R. Subramanian[a], J. Abuthakir[a], L. John Berchmans[b]

[a]PSG College of Technology, Metallurgical Engineering Department, 641 004, Coimbatore, India.
[b]Council of Scientific and Industrial Research (CSIR), Central Electrochemical Research Institute, Electropyro Metallurgy Division, 630003, Karaikudi, India.

Received: June 15, 2022; Revised: March 03, 2023; Accepted: September 25, 2023

$CaZrO_3$and $SrZrO_3$powders were prepared by sol-gel synthesis and plasma sprayed over the Inconel 718 substrate,forming a wear-resistant ceramic coating. X-Ray Diffraction (XRD) analysis of synthesized ceramic powders revealed the presence of $CaZrO_3$and $SrZrO_3$ phases, having an orthorhombic structure. $CaZrO_3$ and $SrZrO_3$powders were sprayed onto the surface of Inconel 718using a plasma spraying process. Scanning Electron Microscope (SEM)analysis of $CaZrO_3$and $SrZrO_3$coated samplesshowedanaveragethickness of about 400µm.Wear depth and wear mechanism for the above sampleswerestudiedusing Pin-on-disc apparatus. Wear results of $CaZrO_3$ and $SrZrO_3$ coated substrates revealed that high wear depths were observed at high speeds and loads. SEM investigations of worn-out samples revealed that both $CaZrO_3$ and $SrZrO_3$ coated samples had undergone delamination wear. $CaZrO_3$ coated samples had exhibitedless delamination and wear depth than $SrZrO_3$ coated samples, thus showing relatively better wear resistance.

Keywords: *Wear-resistant Coatings, Calcium Zirconate, Strontium Zirconate, ceramic coatings, Sol-gel synthesis, Atmospheric plasma spraying.*

1. Introduction

Ceramic oxide coatings are wear-resistant since they are thermodynamically stable at elevated temperatures[1]. Al_2O_3-ZrO_2 has similar wear-resistant nature in addition to high fracture toughness. Zirconia subjected to formation of thermal oxide layer has high tribological wear resistance. However, specific changes in crystal structure cause deterioration in abrasion properties, limiting its applications[2]. Deterioration is usually the presence of defects or impurities in the crystal lattice of the synthesized zirconates. These defects can weaken the material's structural integrity, making it more prone to damage from abrasive forces. Another type of change is the polymorphism of the $CaZrO_3$ and $SrZrO_3$, wherein the structural changes undergoes stability changes. For example, if the crystal lattice of the zirconate becomes distorted or disordered, this can lead to a reduction in its abrasion resistance. Additionally, if the crystal structure undergoes phase transitions at high temperatures or under other extreme conditions, this can also cause deterioration in its abrasion properties. Overall, any changes in the crystal structure of zirconates that result in a reduction in their strength, toughness, or resistance to wear[2-4]. The tribological behaviours of the coatings are assumed to be closely related to their physical and mechanical properties[3-5]. These coatings have applications in orthopedics, cutting tools, biomedical implants, articular head replacement and clinics[3,6]. High plasma power, high-velocity feed andfast deposition time give an optimal process in the case of Titanium dioxide coatings[1]. In general, the ceramic coating materials were prepared by solid-state synthesis, i.e.ball milling method, but the resulting samples contain agglomerated grains of unequal sizes and often contaminated due to impurities incorporated from abrasive particles or incomplete reactions. In contrast to the powder processing methods, the liquid phase processing (e.g., solution-sol-gel technique) provides a molecular-level mixing of the individual **components,** which allowsthe diffusion path in the nanometer range to yield crystalline material at much lower temperatures than generally required for the solid-state reactions[7-12].

$CaZrO_3$ and $SrZrO_3$ are both ceramic oxides of the perovskite family[13]. The process of atmospheric plasma spraying of ceramic coating and various chemical treatments of the prepared ceramic powders were different in the way of their properties and applications from materials synthesized through other routes[6,13]. The atmospheric plasma sprayed ceramic systems such as calcium and strontium zirconates synthesized through chemical methods exhibited significant difference in the particulate nature especially morphologies. Hence the properties of the zirconates prepared through these methods will exhibit different properties when compared to the ceramic systems developed through other synthesis methods and as a result the coating properties will change.The plasma spray distance, plays a significant role in the formation of defect free coatings with higher coating efficiency[14]. The plasma-sprayed coatings using these ceramic powders show better mechanical properties such as indentation crack resistance, adhesion strength and spallation resistance[3,4]. Moreover, coatings are selected with combined properties of ductility, strength and wear resistance.

*e-mail: venkih07@gmail.com

One-step Plasma Electrolytic Oxidation(PEO), micro-arc oxidation and laser cladding are some of the widelyusedprocesses for ceramic powder coatings[2-5,13,15,16]. Recent studies reported that atmospheric plasma spraying (APS) had got relatively high deposition efficiency, flexibility, and formation of uniform microstructures[17-24]. During Atmospheric Plasma Spraying (APS), the ceramic powders are melted at high temperatures up to 1300ºC and sprayed over the substrate[15,19-23,25,26]. APS is a more complicated process, which involves numerous parameters. In this present work, $CaZrO_3$(CZO) and $SrZrO_3$(SZO) were coated over the Inconel 718substrate by the APS technique.Inconel 718 is a high-strength, corrosion-resistant nickel-based superalloy that is commonly used in high-temperature and high-stress applications, such as aerospace and gas turbine engine components[15,16]. It has been a potential choice for coating with ceramic materials due to excellent thermal stability, making it an ideal material for use in high-temperature environments, higher resistant to corrosion and oxidation, even in hostile environments, high wear resistance, such as cutting tools and thermal barrier in various aerospace applications[22,23]. Spraying speed, distance, arc current, powder feed rateand carrier gas flow rate are a few parameters that can be altered in the APS technique[3-5,15,16,26]. Coated substrates were subjected to wear tests using a pin-on-disk tribometer. Wear studies of coated materials using pin-on-disc tribometer revealed that the frictional force is higher in ceramic-metal pair than in ceramic-ceramic pair[3,13]. Coatings deposited byAPStechniquewithhigher particle speedexhibited relatively better abrasion-wear resistance than the coatings deposited by the High-velocity Oxy-fuel process, as reported byWei-Cheng Lih et al.,At higher loads and sliding velocity, the earlier effect of the fatigue and the abrasive effect are present. It is also reported that the debris impact on the worn surface of the samples leads to severe wear. Literatures reveal that primary wear mechanisms are abrasive wear, adhesive wear, severe plastic deformation, and oxidation in samples. Ceramic coatings can improve the wear resistance of metal with carbon nanotube fibers or by lasercladding, which provides a phase-strengthening effect[15].

2. Materials and Methods

2.1. Sol-gel synthesis

Analytical grades of powders (99% purity-Loba chemicals): calcium chloride ($CaCl_2.2H_2O$), strontium chloride ($SrCl_2.2H_2O$), and zirconium oxychloride ($ZrOCl_2.8H_2O$) powders were taken in the stoichiometric ratio for the synthesis of calcium zirconate ($CaZrO_3$) and strontium zirconate ($SrZrO_3$). In addition to the above precursors, EthyleneDiamineTetraAceticacid (EDTA) 0.5N and sodium hydroxide (NaOH) 0.1M were also used for thepreparation of the compounds. A facile sol-gel methodology was adopted to prepare the $CaZrO_3$ and $SrZrO_3$ compounds respectively. The equimolar composition of calcium, strontium and zirconium salt solutions were prepared using distilled water and EDTA was added as a chelating agent. The solutions were mixed at room temperature and NaOH solution (0.1 M) was added to adjust the pH. The prepared gels were then washed with distilled water, dried at 120°C and finally calcined at 1100°C for 8 hours. The crystal structures of the synthesized $CaZrO_3$ and $SrZrO_3$ powder particles were determined using Shimadzu Spectrometer Model XRD 6000 with Cu-Kα as target. Indexing and confirmation of the phases in the powder particles were carried out using the ICDD-PDF2 database.

2.2. Thermal spraying process

The Inconel 718 substrate of dimension (60 mm x 38 mm x 6 mm) was first sand-blasted followed by a degreasing process to ensure a clean surfacebefore the coating process. The coating was prepared by APS (Air Plasma Spray) technique with the standard parameters,as shown in Table 1. Initially, the bond coat of NiCoCrAlYwas coated onto the substrate. The reason for coating a bond coat of NiCoCrAlY onto the Inconel substrate is to provide oxidation and corrosion resistance to the substrate material. The bond coat acts as a barrier layer between the substrate and the topcoat, which typically gives rise to interdiffusion of elements. Over the bond coat, $CaZrO_3$ powders were deposited to achieve a uniform coating thickness of homogenous composition. A similar methodology was adopted for coating $SrZrO_3$ over the substrate. The surface morphology of the powder-coated substrate was analyzed using a JEOL JSM-6360LV Scanning Electron Microscope (SEM).

2.3. Wear analysis

Wear tests were conducted for $CaZrO_3$ and $SrZrO_3$ coated specimens in the Ducompin-on-disc tribometerwith a data acquisition system. Wear tests were carried out following the Design of Experiments(DOE) methodology (L27 orthogonal array). Sliding speed, load and time were chosen as parameters for wear study. In the L27 orthogonal array, three factors with 3 level designs were chosen. Samples were cut to dimensions of8mmx8mmx 6mm. The speed and time of subjection to wear were fed into the device and the load was varied by applying weights. Each experiment was performed by varying these three parameters. After the completion ofthetest, wear depth was determined. Morphology of worn-out surface was analyzed using JEOL JSM-6360LV Scanning Electron Microscope (SEM).

3. Results and Discussion

3.1. XRD analysis of synthesized $CaZrO_3$ and $SrZrO_3$ powders

The ICDD-PDF2 database was used to analyze the XRD pattern obtained for the $CaZrO_3$and $SrZrO_3$ powder samples.

Table 1. Plasma Spray Coating Parameters.

Parameters	Bond Coat	Top Coat 1	Top Coat 2
Current (A)	500	550	550
Voltage (V)	60	70	70
Spraying Distance (mm)	100	100	100
Spraying Speed (mm/sec)	10	10	10
Powder Feed Rate (g/min)	35	35	20
Ar/He Ratio	15/50	15/50	15/50

The XRD patternofcalciumzirconate,as shown in Figure 1a, indicates the presence ofpure $CaZrO_3$ phase, which has an orthorhombic form of crystal structural structure. The lattice parameter of obtained phase was(a = 5.7616 Å, b = 8.0171 Å, c = 5.5912 Å, α = β = γ = 90°) with space group of Pbmn. Crystallite size was determined from X-ray line broadening using Debye Scherer's formula[26]and was found to be 4.80nm.

The XRD pattern of $SrZrO_3$ powder-coated substrate as shown in Figure 1b, reveals the presence of pure $SrZrO_3$phase with a space group of Pbnm lattice parameters of (a = 5.7862 Å, b = 5.8151 Å, c = 8.196 Å, α = β = γ = 90°). The crystallite size was determined from X-ray line broadening using Debye Scherer's formula[26] and found to be 5.20nm.

3.2. SEM analysis of $CaZrO_3$ and $SrZrO_3$coated samples

Figures 2a and 2b showed the SEM images of synthesized $CaZrO_3$ and $SrZrO_3$ samples. It was observed from the SEM micrograph the particles sizes were non-spherical and agglomerated with indistinctive sizes among the powders. The average particle sizes were measured for both $CaZrO_3$ and $SrZrO_3$ samples at 500 X magnification as 98μm and 93μm respectively.

Figure 3a shows the SEM image of as-sprayed $CaZrO_3$ on the **Inconel 718** substrate. It can berevealed that the coating obtained was having an average thickness of 400.33μm. It is also evident from the SEM micrograph that inter-diffusion had occurred between top-coat and bond coat, which leads to strong bonding between them. SEM image of $SrZrO_3$ coated samples shown in Figure 3b, revealed that the coating developed over the substrate was having an average thickness of 400 μm.

3.3. Wear behaviour of$CaZrO_3$ coated sample

Wear results obtained from wear tests of $CaZrO_3$ coated samples are shown in Table 2. It can be revealed thatthe wear depth was higher at high-applied loads, higher speeds and higher sliding times.

Regression equation {Wear (μm) = - 54.9 + 4.14 Load (N) + 0.295 Speed (rpm) + 2.34 Time (minutes)} developed for the analysis of wear for $CaZrO_3$ samples revealed that load is the primary factor in affecting the wear of $CaZrO_3$ coated samples followed by sliding time and sliding speed. It can be inferred from Figure 3, that the $CaZrO_3$ coated sample had attained uniform top coating with fewer asperities. The sound interface achieved in the $CaZrO_3$ coated sampleindicated that an excellent bonding had taken place between the top-coat and substrate.$CaZrO_3$ coated sample exhibited excellent wear resistance at lower loads even though sliding speed and time were increased. Wear studiesindicated that at higher loads and sliding speeds, high compressive forces developed between the asperities of coated sample and disc, caused localizedfragmentation of asperities.This resulted in formation of debris and led to severe wear of coated samples. Wear depth was also found to increase with increasing sliding time and sliding speed.

Figures 4, 5 and 6 revealed that $CaZrO_3$ coated samples had undergone mild delamination at lower load, lowerslidingspeed

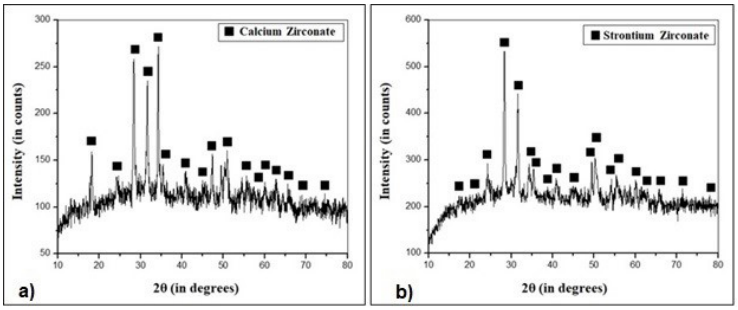

Figure 1. XRD pattern of synthesized $CaZrO_3$(a) and $SrZrO_3$(b).

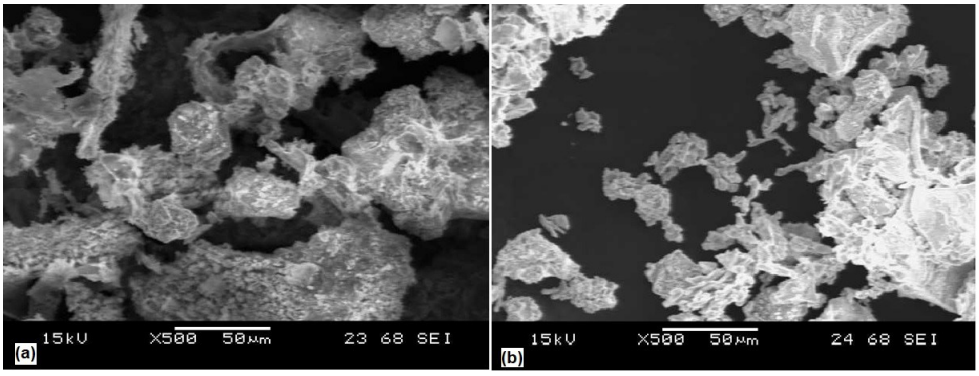

Figure 2.SEM analysis of$CaZrO_3$ (a) and $SrZrO_3$ (b) synthesized powders.

Table 2. Wear test results of $CaZrO_3$ coated samples.

S.No.	Load(N)	Speed(rpm)	Time(minutes)	Wear depth(μm)	Coefficient of friction(μ)
1	10	300	5	92	0.75
2	10	300	10	112	0.51
3	10	300	15	137	0.49
4	10	400	5	120	0.53
5	10	400	10	136	0.57
6	10	400	15	159	0.58
7	10	500	5	140	0.46
8	10	500	10	164	0.46
9	10	500	15	83	0.47
10	15	300	5	98	0.91
11	15	300	10	123	0.91
12	15	300	15	117	0.89
13	15	400	5	132	0.92
14	15	400	10	146	0.80
15	15	400	15	123	0.72
16	15	500	5	187	0.64
17	15	500	10	219	0.63
18	15	500	15	212	0.63
19	20	300	5	102	0.43
20	20	300	10	132	0.40
21	20	300	15	157	0.38
22	20	400	5	165	0.34
23	20	400	10	176	0.32
24	20	400	15	188	0.30
25	20	500	5	162	0.33
26	20	500	10	201	0.30
27	20	500	15	233	0.30

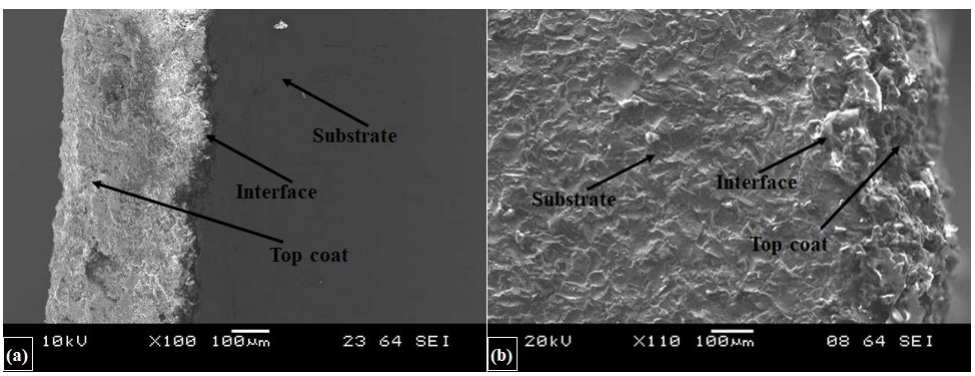

Figure 3. SEM analysis of $CaZrO_3$ (a) and $SrZrO_3$ (b) coated substrate.

and lower sliding time. It can also be observed that mild delamination is transformed into severe delamination at higher loads, speeds and sliding times. It can also be understood from Figures 4, 5 and 6 that at constant sliding speed and sliding time,wear depth wasfound to increase with an increase in load. It is also confirmed that at lower loads, sliding speeds and sliding time of $CaZrO_3$ coated samples had exhibited adhesive wear mechanism. At higher loads, sliding speeds and sliding time $CaZrO_3$ coated samples have undergone the transition from adhesive wear to abrasive wear.

The main effects plot in Figure 7 also revealed that load influenced the wear depth of $CaZrO_3$ coated samples to a larger extent followed by sliding speed. However,with an increase in sliding time wear depth was increasing initially and it was constant after the initial increase in wear depth. This indicated that generation of debris from fragmentation

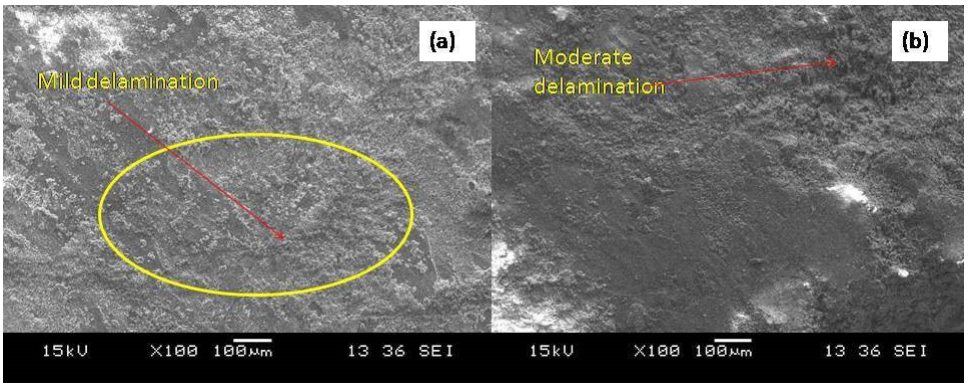

Figure 4. Worn-out surfaces of $CaZrO_3$ coated samples at (a) 10N,300 rpm and 5 minutes (b) 15N,300 rpm and 5minutes.

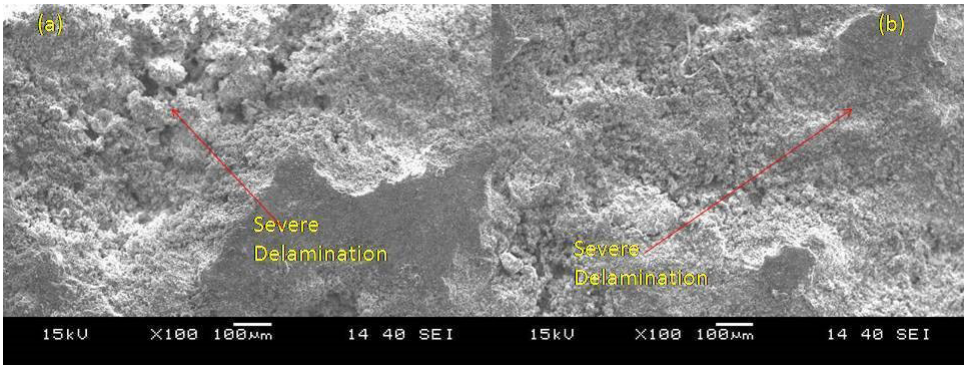

Figure 5. Worn-out surfaces of $CaZrO_3$ coated samples at (a) 15N,400 rpm and 10 minutes (b) 20N,400 rpm and 10minutes.

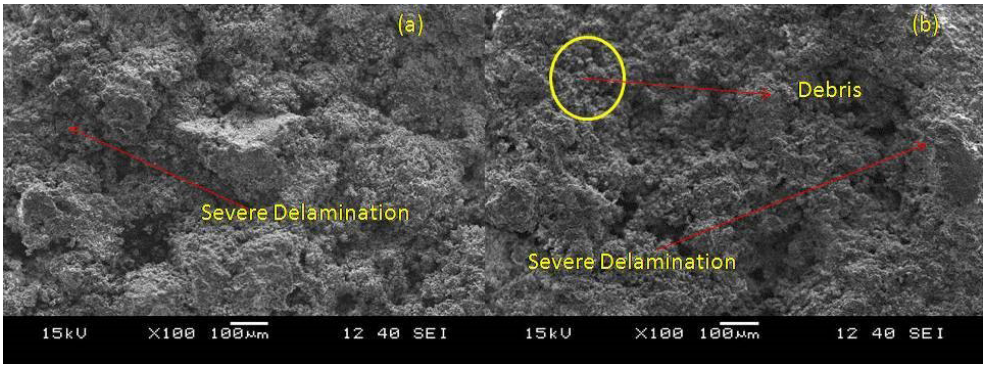

Figure 6. Worn-out surfaces of $CaZrO_3$ coated samples at (a) 15N,500 rpm and 15 minutes (b) 20N,500 rpm and 15minutes.

of asperities at higher load and sliding speed decreased aftera certain sliding time.

3.4. Wear behaviour for $SrZrO_3$coated sample

Wear results obtained from the wear test of $SrZrO_3$samples are shown in Table 3. $SrZrO_3$ coated samples also showed higher wear depths at higher load, higher speed and higher sliding time. However, wear depthwas found to be higher than $CaZrO_3$ coated samples because of the large number of asperities formed on the topcoat layer.

Regression equation for the analysis of wear of $SrZrO_3$ coated samples {Wear (µm) = - 303 + 9.62 Load (N) + 0.884 Speed (rpm) + 6.47 Time (minutes)} also indicated that wear depths are higher at higher loads, higher speed and higher sliding time.

Figures 8, 9 and 10 reveal that $SrZrO_3$ coated samples had undergone severe delamination than $CaZrO_3$ coated samples at all levels of load, sliding speed and sliding time. This severe delamination can also be attributed to formation of higher amount ofdebrisinthecontactregion.At

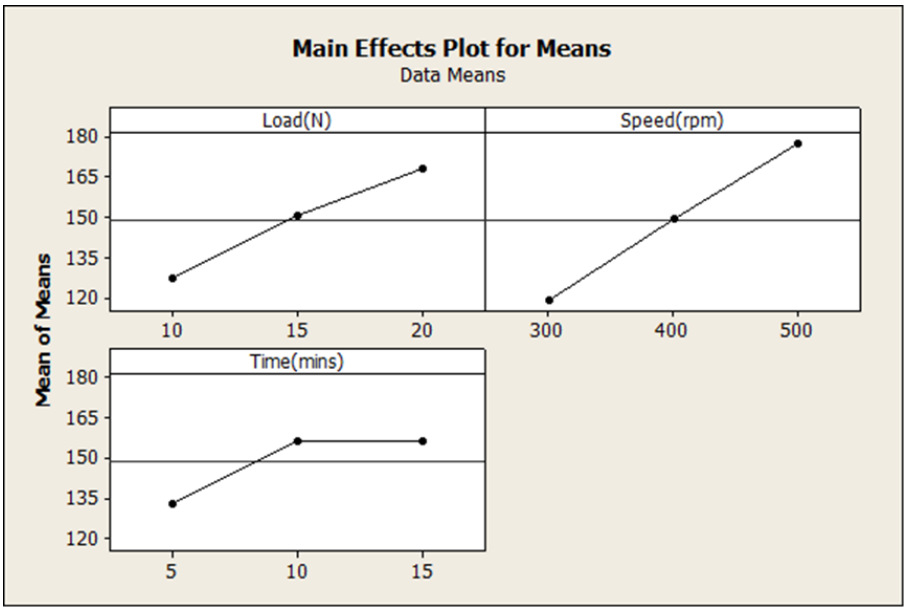

Figure 7. Main Effects plot for means of wear values of $CaZrO_3$ coated samples.

Table 3. Wear results of $SrZrO_3$ coated samples.

S.No.	Load (N)	Speed (rpm)	Time (minutes)	Wear depth (μm)	Coefficient of friction(μ)
1	10	300	5	147	0.73
2	10	300	10	153	0.71
3	10	300	15	164	0.65
4	10	400	5	166	0.61
5	10	400	10	189	0.55
6	10	400	15	214	0.41
7	10	500	5	178	0.49
8	10	500	10	193	0.45
9	10	500	15	229	0.44
10	15	300	5	181	0.68
11	15	300	10	197	0.65
12	15	300	15	207	0.62
13	15	400	5	243	0.69
14	15	400	10	267	0.65
15	15	400	15	294	0.61
16	15	500	5	274	0.57
17	15	500	10	282	0.55
18	15	500	15	309	0.53
19	20	300	5	211	0.42
20	20	300	10	228	0.40
21	20	300	15	246	0.36
22	20	400	5	299	0.33
23	20	400	10	341	0.32
24	20	400	15	387	0.32
25	20	500	5	426	0.30
26	20	500	10	450	0.28
27	20	500	15	468	0.27

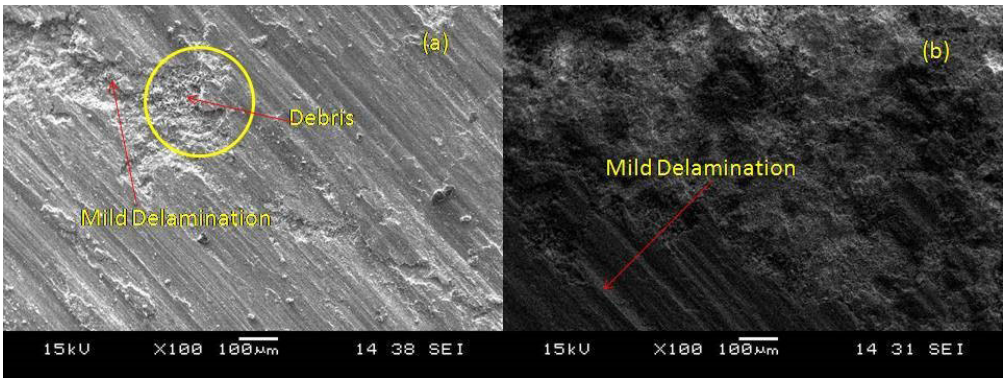

Figure 8. Worn-out surfaces of $SrZrO_3$ coated samples at (a) 10N,300 rpm and 5 minutes (b) 15N,300 rpm and 5minutes.

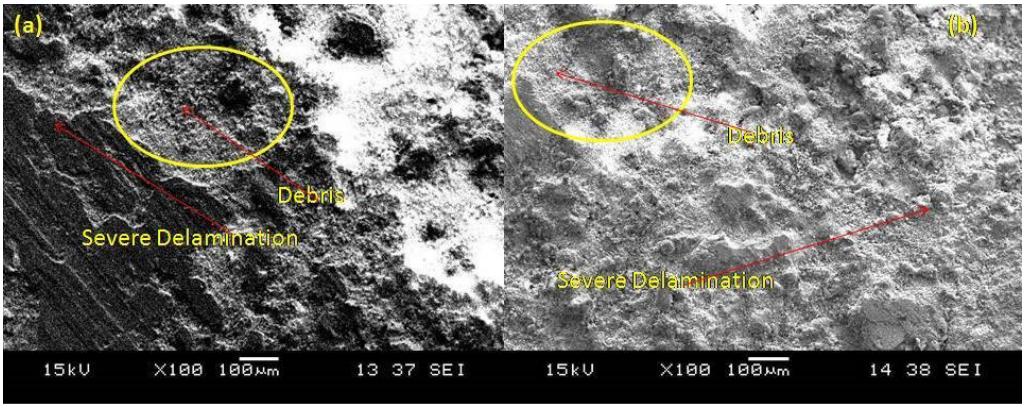

Figure 9. Worn-out surfaces of $SrZrO_3$ coated samples at (a) 15N,400 rpm and 10 minutes (b) 20N,400 rpm and 10minutes.

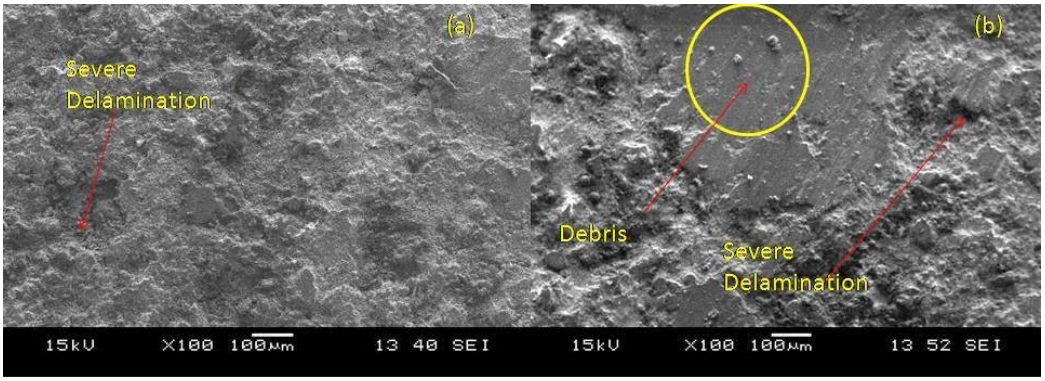

Figure 10. Worn-out surfaces of $SrZrO_3$ coated samples at (a) 15N,500 rpm and 15 minutes (b) 20N,500 rpm and 15minutes.

higher levels ofload,speed and time due to the formation of higher amount of localized debris,wear depth was much severe than the wear of $CaZrO_3$ coated samples. In $SrZrO_3$ coated samples also, wear depth increased with an increase in load at constant sliding speed and sliding time as indicated in Figures 8, 9 and 10. $SrZrO_3$ coated samples also had undergone transition from adhesive wear to abrasive wear at higher loads, sliding speeds and sliding time.

The main effects plot of $SrZrO_3$coated samples in Figure 11 indicated that load had got major influence in affecting the wear resistance of the samples. The wear depth

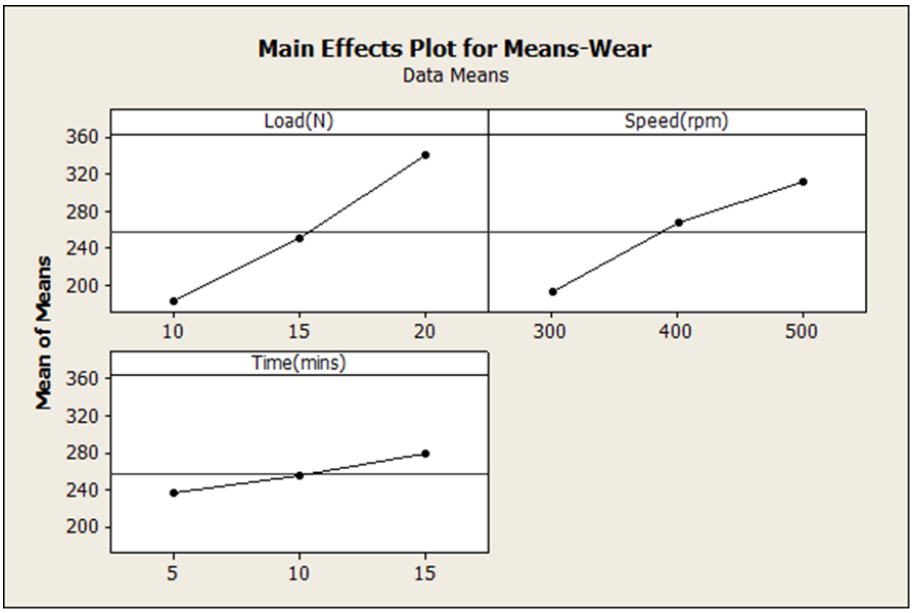

Figure 11. Main Effects plot for means of wear values of $SrZrO_3$ coated samples.

of the $SrZrO_3$ coated sample increased with an increase in sliding time due to the formation of a large number of debris compared with $CaZrO_3$ coated samples.

4. Conclusion

The synthesized powders of Calcium zirconate and Strontium zirconate were coated ontheInconel 718 substrate with an intermediate layer of NiCoCrAlY as a bond coat. SEM analysis of $CaZrO_3$ and $SrZrO_3$coated samples revealed that the coating was consistent in terms of thickness. SEM analysis also revealed that $CaZrO_3$ coating was much more uniform with fewer asperities and $SrZrO_3$ coating was non-uniform with numerous asperities. Wear behaviour of $CaZrO_3$ and $SrZrO_3$ coated samples revealed that the wear rate of the $SrZrO_3$sample was comparatively higher than the $CaZrO_3$ coated sample. It was evident that the wear rate increases with an increase inload and speedfor $CaZrO_3$and $SrZrO_3$coatedsamples due to the formationofasperities. SEM investigations of worn-out samples indicated that both samples exhibited delamination wear mechanisms. SEM investigations of worn-out samples indicated that both $CaZrO_3$ and $SrZrO_3$ samples exhibited a transition from adhesive to abrasive wear mechanism at higher loads, sliding speeds and sliding time.However, the $CaZrO_3$ coated sample had exhibited less delamination & wear rate than the $SrZrO_3$ coated samples because localized asperities and existing asperities in the $SrZrO_3$ coated sample had caused relatively higher wear and delamination than $CaZrO_3$ coated sample.

5. References

1. Forghani SM, Ghazali MJ, Muchtar A, Daud AR, Yusoff NHN, Azhari CH. Effects of plasma spray parameters on TiO2-coated mild steel using design of experiment (DoE) approach. Ceram Int. 2013;39:3121-7.
2. Zhang L, Zhang W, Han Y, Tang W. Ananoplate-like α-Al_2O_3 out-layered Al_2O_3-ZrO_2 coating fabricated by micro-arc oxidation for hip joint prosthesis. Appl Surf Sci. 2016;361:141-9.
3. Ageh V, Choudhuri D, Scharf TW. High frequency reciprocating sliding wear behavior and mechanisms of quaternary metal oxide coatings. Wear. 2015;330:390-9.
4. Dyshlovenko S, Pawlowski L, Roussel P, Murano D, Le Maguer A. Relationship between plasma spray operational parameters and microstructure of hydroxyapatite coatings and powder particles sprayed into water. Surf Coat Tech. 2005;200:3845-55.
5. Chandler CD, Roger C, Hampden-Smith MJ. Chemical aspects of solution routes to perovskite-phase mixed-metal oxides from metal-organic precursors. Chem Rev. 1993;93:1205-41.
6. Hench LL, West JK. The sol-gel process. Chem Rev. 1990;90:33-72.
7. Uchino K, Sadanaga E, Hirose T. Dependence of the crystal structure on particle size in barium titanate. J Am Ceram Soc. 1989;72:1555-8.
8. Phule PP, Risbud SH. Low-temperature synthesis and processing of electronic materials in the BaO-TiO2 system. J Mater Sci. 1990;25:1169-83.
9. Beck HP, Mueller F, Haberkorn R, Wilhelm D. Synthesis of perovskite type compounds via different routes and their X-ray characterization. Nanostruct Mater. 1995;6:659-62.
10. Karabas M, Bal E, Kilic A, Taptık IY. Effect of air plasma spray parameters on the properties of YSZ and CYSZ thermal barrier coatings. J Aust Ceram Soc. 2016;52:175-82.
11. Li QH, Savalani MM, Zhang QM, Huo L. High temperature wear characteristics of TiC composite coatings formed by laser cladding with CNT additives. Surf Coat Tech. 2014;239:206-11.
12. Liu XB, Liu HQ, Meng XJ, Sun CF, Wang MD, Qi LH, et al. Effects of aging treatment on microstructure and tribological properties of nickel-based high-temperature self-lubrication wear resistant composite coatings by laser cladding. Mater Chem Phys. 2014;143:616-21.
13. Kotlan J, Pala Z, Musalek R, Ctibor P. On reactive suspension plasma spraying of calcium titanate. Ceram Int. 2016;42:4607-15.
14. Khalid M, Mujahid M, Nusair Khan A, Rawat RS, Mehmood K. Effect of arc current on microstructure, texturing and wear behavior of plasma sprayed CaZrO3 coating. Ceram Int. 2013;39:2293-302.

15. Niranatlumpong P, Sukonkhet C, Ninon K. Loss of Y from NiCrAlY powder during air plasma spraying. Surf Coat Tech. 2015;280:277-81.
16. Sreedhar G, Masroor Alam MD, Raja VS. Hot corrosion behaviour of plasma sprayed YSZ/Al_2O_3 dispersed NiCrAlY coatings on Inconel-718 superalloy. Surf Coat Tech. 2009;204:291-9.
17. Mishra SC, Praharaj S. Plasma spray deposition of fly ash onto mild steel substrates using a fractional factorial design approach. Orrisa Journal of Physics. 2011;18:199-206.
18. Wu Z. Empirical modeling for processing parameters' effects on coating properties in plasma spraying process. J Manuf Process. 2015;19:1-13.
19. Wang C, Wang Y, Fan S, You Y, Wang L, Yang C, et al. Optimized functionally graded $La_2Zr_2O_7$/8YSZ thermal barrier coatings fabricated by suspension plasma spraying. J Alloys Compd. 2015;649:1182-90.
20. Mishra SC. Analysis of experimental results of plasma spray coatings using statistical techniques. In: Jazi HS. Advanced plasma spray applications. London: Intech; 2012. p. 84-96.
21. Levingstone TJ, Ardhaoui M, Benyounis K, Looney L, Stokes JT. Plasma sprayed hydroxyapatite coatings: understanding process relationships using design of experiment analysis. Surf Coat Tech. 2015;283:29-36.
22. Silva A, Booth F, Garrido L, Aglietti E, Pena P, Baudín C. Influence of phase composition on the sliding wear of composites in the system $CaZrO_3$–MgO–ZrO_2against ZrO_2 and steel. Theor Appl Fract Mech. 2016;85:125-33.
23. Liang B, Zhang G, Liao H, Coddet C, Ding C. Friction and wear behavior of ZrO_2–Al_2O_3 composite coatings deposited by air plasma spraying: correlation with physical and mechanical properties. Surf Coat Tech. 2009;203:3235-42.
24. Chen TC, Chou CC, Yung TY, Cai RF, Huang JY, Yang YC. A comparative study on the tribologicalbehavior of various thermally sprayed Inconel 625 coatings in a saline solution and deionized water. Surf Coat Tech. 2020;385:125442.
25. Yin B, Peng Z, Liang J, Jin K, Zhu S, Yang J, et al. Tribological behavior and mechanism of self-lubricating wear-resistant composite coatings fabricated by one-step plasma electrolytic oxidation. Tribol Int. 2016;97:97-107.
26. Scherrer P. Nanoscience and the Scherrer equation versus the 'Scherrer–Gottingen equation. 1918;2:98-100. http://dx.doi.org/10.1590/sajs.2013/a0019.